Manifestation of spin-charge fluctuations in the spectral and thermodynamic properties of quasi-two-dimensional rare-earth intermetallic compounds

Cite as: Low Temp. Phys. **43**, 191 (2017); https://doi.org/10.1063/1.4977211
Submitted: 01 August 2016 . Accepted: 10 February 2017 . Published Online: 15 March 2017

V. V. Val'kov, and A. O. Zlotnikov

Manifestation of spin-charge fluctuations in the spectral and thermodynamic properties of quasi-two-dimensional rare-earth intermetallic compounds

V. V. Val'kov[a)] and A. O. Zlotnikov

Kirensky Institute of Physics, Krasnoyarsk Scientific Center of the Siberian Branch of the RAS, 50-38, Akademgorodok, Krasnoyarsk 660036, Russia

(Submitted August 1, 2016)
Fiz. Nizk. Temp. **43**, 233–244 (February 2017)

In the framework of the modified periodic Anderson model with exchange interaction in the subsystem of localized states, it is shown that spin-charge fluctuations in quasi-two-dimensional intermetallic compounds with rare-earth ions in the mixed valence state significantly affect both the spectrum of magnetic excitations and the conditions at which the antiferromagnetic phase is realized. The spectral characteristics of the phase were obtained by the method of the diagram technique for Hubbard operators in the one-loop approximation, which allows to account for the spin-charge fluctuation contributions to the components of the mass and the force operators. The developed theory allowed to quantitatively describe the pressure dependence of the Néel temperature observed in a quasi-two-dimensional antiferromagnetic heavy-fermion intermetallic compound $CeRhIn_5$. *Published by AIP Publishing.* [http://dx.doi.org/10.1063/1.4977211]

1. Introduction

Significant interest in the properties of heavy-fermion antiferromagnets is due to unusual superconductivity realized in these compounds, quantum phase transitions, as well as a strongly pronounced competition between the tendency to magnetic ordering and the Kondo fluctuations. The quantum phase transitions are triggered by an external or chemical pressure and accompanied by qualitative changes in the structure of the ground state and, accordingly, in the observed characteristics. For example, in heavy-fermion metals $CeCu_{6-x}Au_x$ and $YbRh_2Si_2$, a passage through the quantum critical point upon varying the control parameters, such as the doping level x and the magnetic field, is accompanied by the destruction of the long-range antiferromagnetic (AFM) order.[1] Cerium compounds, such as $CePd_2Si_2$, $CeIn_3$,[2] $CeRhIn_5$,[3] and $CePt_2In_7$,[4] exhibit superconductivity in the vicinity of the proposed quantum critical point under pressure.

The mechanism of magnetic ordering remains one of the main problems in the physics of heavy-fermion systems. It is well known that the long-range AFM order arising due to the indirect Ruderman-Kittel-Kasuya-Yoshida (RKKY) exchange interaction and the Kondo fluctuations are competing with each other.[5] Thus, the rare-earth compounds are generally described in terms of the Kondo model, in which the type of the ground state depends on the outcome of the above competition: either a state with the long-range magnetic order (most often antiferromagnetic) or a nonmagnetic metallic state. In this scenario, simultaneously with the destruction (emergence) of the long-range AFM order in the quantum critical point, the Kondo regime can emerge (break) and the transition from localized to delocalized electrons is realized.[6,7] It should be noted that heavy-fermion systems at the quantum critical point exhibit anomalous features such as the divergence of the effective electron mass and an abrupt expansion of the Fermi surface. These anomalies cannot be described in terms of the Hertz-Millis theory of the quantum phase transitions for band magnets.

The above competition scenarios do not take into consideration the fact that 4*f*-electrons in the AFM phase are quasi-localized and form a coherent heavy-fermion state. The existence of such a state is indicated by experimental data showing that, for example, in the AFM phase of $CeRhIn_5$ the effective and cyclotron masses of electrons are much greater than the mass of free electrons.[8,9] In Ref. 10 it has been suggested that a mixed-valence regime is realized in this compound. In this respect, it appears natural to describe the formation of magnetic ordering within the framework of the periodic Anderson model taking into account a strong coupling between the spin and charge degrees of freedom in the regime where the bare localized level and the Fermi level are close to each other. It is essential that this approach allows to describe both strong renormalization of the electron mass and changes in the topology of the Fermi surface at the quantum critical point without involving the scenario based on breaking the Kondo regime.[11–13]

It should be noted that in Ref. 14, the Stoner criterion has been analyzed on the background of the Kondo state in the systems with strong orbital degeneracy of the *f*-level. Using an approach based on the introduction of auxiliary fermions to preserve the commutation rules, it has been shown that quantum fluctuations lead to the realization of a weak itinerant antiferromagnetism (of the spin-density wave type). At the same time due to the hybridization, a weak antiferromagnetism is also induced in the localized subsystem. However, the mixed valence regime has not been considered so far.

The study of the formation conditions of the AFM ordering in the periodic Anderson model has been carried out earlier in the Hartree-Fock approximation,[15] as well as by using the method of slave bosons.[16,17] However, it should be emphasized that in the above mean-field approaches, the Néel temperature T_N is low only in the vicinity of the quantum phase transitions in the parameter V describing the hybridization between the itinerant and localized electrons

or in the parameter U of the intra-atomic Coulomb repulsion of the localized electrons. This means that even small changes in the environmental conditions (such as pressure) are capable of inducing the quantum phase transition from AFM to the paramagnetic (PM) phase. Meanwhile, in many heavy-fermion compounds, despite the fact that their T_N does not exceed several kelvin, antiferromagnetism is sufficiently resistant to pressure. For example, in $CeRhIn_5$ with $T_N = 3.8$ K, the Néel temperature first increases with increasing the pressure, then there is a linear decline, and only at a pressure of about 20 kbar, the antiferromagnetism is destroyed.

An alternative approach to describe the magnetism in these systems is related to the calculation of the dynamic magnetic susceptibility. The magnetic susceptibility determined in the PM phase allows to find the temperature of the instability with respect to the formation of one or another type of magnetic ordering. The problem of determining the dynamic magnetic susceptibility directly in the AFM phase requires solving the self-consistent equations allowing to find both the temperature dependence of the AFM order parameter and the Néel temperature. Earlier, the dynamic magnetic susceptibility in the PM phase of the periodic Anderson model has been calculated using the decoupling method for the equations of motion of the irreducible Green's functions[18] and in the framework of the random phase approximation[19] in the limit of weak Coulomb interaction. The use of the perturbation theory with respect to the hybridization interaction for calculating the dynamic magnetic susceptibility has been proposed in Ref. 20. It has been shown that in the mixed valence regime, the effective interaction due to the hybridization between the localized and itinerant electrons suppresses any magnetic fluctuations. In the limit $U \to \infty$ limit, a method of calculating the dynamic magnetic susceptibility based on the diagram technique for Hubbard operators within the framework of the Hubbard model and the t-J model has been developed.[21] In Ref. 22, using this approach, the dynamic magnetic susceptibility in the PM phase of the periodic Anderson model has been determined for $U \to \infty$.

Many cerium compounds with heavy fermions, such as $Ce_nT_mIn_{3n+2m}$ compounds,[23] have a quasi-two-dimensional (quasi-2D) structure, schematically shown in Fig. 1. It is known that for a quasi-2D Heisenberg antiferromagnet, the Néel temperature in the Tyablikov approximation is given by $T_N = \pi J/[\ln(J/K) + c]$, where J is the exchange parameter between the nearest ions in the xy plane, the parameter K determines the magnitude of the exchange interaction between the nearest neighbors along the z-axis ($K \ll J$) and c is the constant depending on the lattice type.[24] The above equation indicates a lowering of the transition temperature as compared to the case of spatially isotropic exchange coupling. For $CeRhIn_5$ compound, based on neutron spectroscopy data, the exchange parameters for Ce ions have been estimated as $J = 0.74$ meV and $K = 0.1$ meV.[25] In Ref. 25, the weak exchange between next-nearest neighbors along the z-axis has also been taken into account, which allowed to describe the incommensurate magnetic structure at atmospheric pressure. Since the AFM structure of $CeRhIn_5$ becomes commensurate,[26] long-range exchange parameters can be neglected in this case.

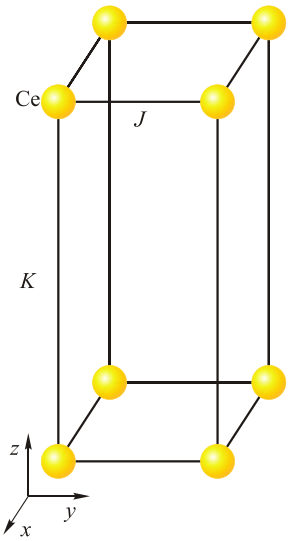

FIG. 1. Schematic representation of the structure of the quasi-two-dimensional Ce115-compounds. J and K denote the parameters of the exchange interaction between Ce-ions.

For the rare-earth intermetallic compounds with magnetic ordering, it is important that in the most interesting case of the regime of strong electron correlations as well as in the case of the energy of single-electron excitation close to the Fermi level (the situation of mixed valence), the hybridization processes can be separated into high-energy and low-energy.[27] The former include the transitions in which, due to the strong correlation, the energy of the system changes by an amount much larger than the hybridization coupling parameter. The presence of such a large energy difference allows to account this hybridization interaction within the operator form of the perturbation theory in the atomic representation and to obtain the effective Hamiltonian describing, in particular, the exchange coupling between the quasi-localized states of the rare-earth ions. The parameter of this interaction is given by the expression $J \sim V^4/U^3$, where U is the energy of intra-atomic repulsion and V is the intensity of the hybridization between localized and itinerant electrons. The remaining low-energy hybridization contributions determine the properties of the mixed-valence regime. Note that in the Ce115 compounds (e.g., $CeRhIn_5$) the role of localized electrons is played by Ce 4f-electrons, while the itinerant state is formed mainly by p-electrons of In.

In view of the above peculiarities of the electronic structure of rare-earth intermetallic compounds, in the present work, on the basis of the extended periodic Anderson model that explicitly takes into account the exchange interaction between the 4f-electrons, we investigated the AFM phase of quasi-2D heavy-fermion cerium intermetallic compounds. To obtain the self-consistency equations, the diagram technique for Hubbard operators was applied. The calculation of the transverse spin Green's function was carried out in the one-loop approximation, allowing to obtain the expressions for the components of mass and force operators, taking into account the contribution of spin-charge fluctuations. The effective interaction between quasi-localized electrons promotes the formation of the AFM state, while the hybridization interaction between the localized and itinerant electron

subsystems is considered as a perturbation. It was shown that in this approach, long-range AFM ordering in the mixed-valence regime can be realized. Numerical solution of the self-consistent equations allowed us to obtain the pressure dependence of the Néel temperature for quasi-2D cerium intermetallic compounds. This dependence is not only in qualitative agreement with the experimental data[3] but also provides quantitatively good description. It was found that low-energy hybridization processes are responsible for the destruction of antiferromagnetism. Furthermore, two contributions affecting the realization of magnetic ordering can be separated: super-exchange coupling of the 4*f*-electrons promotes long-range AFM order, while spin-charge fluctuations caused by the low-energy hybridization processes of *f*- and *p*-electrons can either contribute to antiferromagnetism or suppress it. The partial contributions of these microscopic mechanisms to the effective parameters of the exchange interactions in $CeRhIn_5$ were estimated.

2. Extended Anderson model in the atomic representation

The Hamiltonian of the extended periodic Anderson model which takes into account the superexchange interaction between the 4*f*-electrons and uses the two-sublattice description for the quasi-2D electron structure can be represented as

$$\hat{\mathcal{H}}_{\text{eff}} = \hat{\mathcal{H}}_0 + \hat{\mathcal{H}}_{\text{mix}} + \hat{\mathcal{H}}_{\text{exch}}. \tag{1}$$

The first term describes non-interacting localized and itinerant electrons

$$\hat{\mathcal{H}}_0 = \sum_{j=1,2}\Big\{\sum_{k\sigma}\xi_{\alpha k}\alpha^{\dagger}_{jk\sigma}\alpha_{jk\sigma} + \sum_{k\sigma}\xi_{\beta k}\beta^{\dagger}_{jk\sigma}\beta_{jk\sigma} + \sum_{f\sigma}\xi^{F}_{\sigma}X^{\sigma\sigma}_{jf} + \sum_{g\sigma}\xi^{G}_{\sigma}Y^{\sigma\sigma}_{jg}\Big\}. \tag{2}$$

$\hat{\mathcal{H}}_{\text{mix}}$ is the operator of the hybridization interaction between the localized and itinerant electrons

$$\hat{\mathcal{H}}_{\text{mix}} = \sum_{j,k\sigma}\frac{1}{\sqrt{2}}\Big\{(V_k + W_k)\alpha^{\dagger}_{jk\sigma}(X_{jk\sigma} + Y_{jk\sigma}) + (W_k - V_k)\beta^{\dagger}_{jk\sigma}(X_{jk\sigma} - Y_{jk\sigma})\Big\} + \text{h.c.} \tag{3}$$

The effective AFM coupling between the localized electrons is determined by the third term of the Hamiltonian

$$\hat{\mathcal{H}}_{\text{exch}} = \sum_{j}\sum_{\langle fg\rangle}J_{fg}\left(\mathbf{S}_{jf}\mathbf{S}_{jg} - \frac{1}{4}\hat{N}_{jf}\hat{N}_{jg}\right) + \sum_{i\neq j}\sum_{\langle fg\rangle}K_{fg}\left(\mathbf{S}_{if}\mathbf{S}_{jg} - \frac{1}{4}\hat{N}_{if}\hat{N}_{jg}\right). \tag{4}$$

Here, to describe the quasi-two-dimensionality of rare-earth intermetallic compounds we introduced summation over the index $j = 1, 2$, which enumerates the planes along the *z*-axis of the unit cell. We consider the AFM structure of the *G*-type. The operators $\alpha_{jk\sigma}$ and $\beta_{jk\sigma}$ describe the Bogolyubov quasiparticles formed in the itinerant electron subsystem due to the transition to the two-sublattice representation. The seed energies of quasiparticles are determined by the expressions $\xi_{\alpha k} = \xi_k + \Gamma_k$ and $\xi_{\beta k} = \xi_k - \Gamma_k$, where $\xi_k = \varepsilon_0 + t_k - \mu$, ε_0 is the single-site energy of an itinerant electron, μ is the chemical potential, and the functions t_k and Γ_k are defined as Fourier transforms of the hopping integrals within a single sublattice and between the sublattices, respectively. It is assumed that hopping is only possible in the *xy* plane.

The localized 4*f*-electrons belonging to the site *l* are described in the atomic representation using the Hubbard operators $X^{nn'}_{l} = |n;l\rangle\langle l;n'|$, where $|n;l\rangle$ is one of the atomic states. The state $|0;l\rangle$ defines the state without localized electrons on the site *l*. The state with one electron at a site having the spin projection $\sigma = \uparrow,\downarrow$ is denoted $|\sigma,l\rangle$. Sites marked with the index *f* are related to the *F*-sublattice, for which, in the presence of antiferromagnetism, $\langle S^{z}_{jf}\rangle = R > 0$. The *G*-sublattice sites are enumerated with the index *g*, and for them the equality $\langle S^{z}_{jg}\rangle = -R$ holds. The bare energy of an 4*f*-electron is renormalized given the self-consistent mean-field $\xi^{F}_{\sigma} = E_0 - \mu - (J_0 + K_0)n_L/4 - \eta_\sigma\tilde{h}$, $\tilde{h} = (J_0 + K_0)R/2$, $\xi^{G}_{\sigma} = \xi^{F}_{\sigma}$, where n_L is the average number of localized electrons at a site, $J_0 = 4J$, $K_0 = 2K$. The function η_σ, which depends on σ, is determined in the usual way: $\eta_\sigma = 1$ for $\sigma = \uparrow$ and $\eta_\sigma = -1$ for $\sigma = \downarrow$.

In the term $\hat{\mathcal{H}}_{\text{mix}}$, the quantities V_k and W_k denote the Fourier transforms of the hybridization integrals in the *xy*-plane for the electrons located within the same sublattice or between the sublattices, respectively.

The magnitudes of the exchange interaction between the localized electrons in the *xy*-plane and along the *z*-axis are given by the parameters J_{fg} and K_{fg}, respectively. It is assumed that the exchange interaction occurs only between nearest neighbors. This is reflected by placing the site indices *f* and *g* at the summation sign into angle brackets. $\mathbf{S}_{jm}$ is the quasi-spin vector operator of the localized subsystem, the components of which are associated with the operators of the atomic representations through the equations $S^{+}_{jm} = X^{\uparrow\downarrow}_{jm}$, $S^{-}_{jm} = X^{\downarrow\uparrow}_{jm}$ and $S^{z}_{jf} = \sum_\sigma(\eta_\sigma/2)X^{\sigma\sigma}_{f}$. The operator of the number of localized electrons on the site *f* is defined as $\hat{N}_{jf} = \sum_\sigma X^{\sigma\sigma}_{jf}$.

3. Mass and force operators for the transverse spin Green's function

To find the spectrum of magnetic excitations with spin-charge fluctuations taken into account and to obtain the self-consistent equation in the AFM phase, we use the diagram technique for Hubbard operators.[28,29] Let us introduce the transverse spin Matsubara Green's function in the atomic representation

$$D^{Aj,Bj_1}_{\perp}(m\tau;m'\tau') = -\langle T_\tau X^{\uparrow\downarrow}_{jm}(\tau)X^{\downarrow\uparrow}_{j_1m'}(\tau')S(\beta)\rangle_{0,c}, \tag{5}$$

describing the magnetic properties of the system. The time-dependent Hubbard operators are written in the interaction representation and T_τ is the time ordering operator. The notation "*Aj*" is introduced to show that the Hubbard operator which stands first in the definition of the Green's function refers to the plane *j* of the unit cell and belongs to a particular sub-lattice: $A = F$ for $\mathbf{R}_m = \mathbf{R}_f$, and $A = G$ for $\mathbf{R}_m = \mathbf{R}_g$. Similarly, the index Bj_1 uniquely determines to which sublattice and plane the second operator of the Green's function belongs. Averaging is carried out over the statistical

ensemble defined by the Hamiltonian $\hat{\mathcal{H}}_0$. The scattering matrix has the usual form

$$S(\beta) = T_\tau \exp\left(-\int_0^\beta \hat{\mathcal{H}}_{\rm int}(\tau)d\tau\right),$$

where the interaction operator $\hat{\mathcal{H}}_{\rm int}$ includes the operators of hybridization and exchange interactions and $\beta = 1/T$ is the inverse temperature.

Fourier transformation and expansion in quasi-momenta of the Matsubara Green's function can be written as

$$D_\perp^{Aj,Bj_1}(m\tau; m'\tau') = \frac{T}{N}\sum_{\mathbf{q},\omega_l} e^{i\mathbf{q}(\mathbf{R}_m - \mathbf{R}_{m'}) - i\omega_l(\tau-\tau')} D_\perp^{Aj,Bj_1}(\mathbf{q}, i\omega_l), \tag{6}$$

where $i\omega_l$ are the even Matsubara frequencies. In what follows, a four-vector $q = (\mathbf{q}, i\omega_l)$ will be used.

For contracted notation, we introduce the matrix Green's function $\hat{D}_\perp$ in the block form

$$\hat{D}_\perp = \begin{bmatrix} \hat{D}_\perp^{FF} & \hat{D}_\perp^{FG} \\ \hat{D}_\perp^{GF} & \hat{D}_\perp^{GG} \end{bmatrix}, \quad \hat{D}_\perp^{AB} = \begin{bmatrix} D_\perp^{A1,B1}(q) & D_\perp^{A1,B2}(q) \\ D_\perp^{A2,B1}(q) & D_\perp^{A2,B2}(q) \end{bmatrix}. \tag{7}$$

This function can be written through the product $\hat{D}_\perp = \hat{G}_\perp \hat{P}$, where $\hat{P}$ is the matrix of the force operator components.[30,31] The Dyson equation for the matrix function $\hat{G}_\perp$ is

$$\hat{G}_\perp = \hat{G}_\perp^{(0)} + \hat{G}_\perp^{(0)}\hat{\Sigma}\hat{G}_\perp, \tag{8}$$

where the function $\hat{G}_\perp^{(0)}$ is determined via the force operator from the equation

$$\hat{G}_\perp^{(0)} = \hat{G}^{(0)} + \hat{G}^{(0)}\hat{P}\hat{I}\hat{G}_\perp^{(0)}. \tag{9}$$

The components of the diagonal matrix function $\hat{G}_\perp^{(0)}$ determine the bare quasi-spin Green's function for the F- and G-sublattices, $\hat{\Sigma}$ is the matrix mass operator and $\hat{I}$ is the matrix composed of the Fourier transforms of the exchange integrals.

If the localized level is completely filled (the Fermi level lies above the f-level), the system is close to the behavior of the Heisenberg antiferromagnet. In this case, the long-range AFM order is completely determined by the effective exchange interaction in localized subsystem. In the case of partially filled localized level (but close to the regime of $n_L = 1$), the renormalizations associated with spin-charge fluctuations become important. These renormalizations are manifested in the main characteristics of the antiferromagnet such as the spectrum of the spin-wave excitations, the AFM order parameter and the Néel temperature. In what follows, we will account for the contributions of the exchange interaction in Eqs. (8) and (9) in the simplest loop-free approximation (Tyablikov's approximation). In this case, only the corrections due to the hybridization interaction in the one-loop approximation will be considered for the mass and force operators.[32]

Figures 2 and 3 show the types of diagrams for arbitrary components A_jB_j of the matrix mass and force operators,

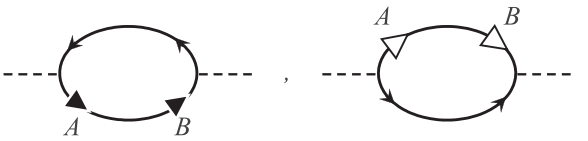

FIG. 2. One-loop diagrams for the AB-component of the mass operator of the transverse spin Green's function.

respectively. The diagrams were obtained using the principle of topological continuity.[33] It should be noted that the expressions do not depend on the plane number j in the quasi-2D unit cell, since the hybridization is only possible in the xy-plane, and this index will be omitted in what follows. The solid lines with two arrows, ▷ or ▶, represent the propagators in the Hubbard-I approximation of localized electrons with spin projections ↑ and ↓, respectively, in the two-sublattice representation. Bare Green's functions of f-electrons are indicated by solid lines with one arrow ▷ (▶). The solid lines with two thin arrows identify any of the four propagators for itinerant electrons produced when switching to the Bogolyubov operators. The point where different lines in the diagram intersect indicates the presence of a hybridization interaction. The symbols ○ and ● denote the Hubbard end factors $F_{A\sigma} = \langle X_m^{00} + X_m^{\sigma\sigma}\rangle$ for the respective directions of electron spin, where the site m belongs to the sublattice A. The total number of diagrams for the mass and force operators in the one-loop approximation, taking into account the two-sublattice structure, is 64.

Relating the graphs to analytical expressions, we obtain an explicit form for the components of the mass and force operators

$$\Sigma^{AB}(q) = -\frac{T}{2N}\sum_p \Big[G_{0\downarrow,0\downarrow}^{AB}(q+p)L_\uparrow^{BA}(p) + G_{\uparrow0,\uparrow0}^{AB}(q-p)L_\downarrow^{AB}(p)\Big], \tag{10}$$

$$\delta P^{AB}(q) = -\frac{T}{2N}\sum_p \Big[G_{0\downarrow,0\downarrow}^{AB}(q+p)G_{0\uparrow}^{(0)B}(p)F_{B\uparrow}L_\uparrow^{BA}(p) - G_{\uparrow0,\uparrow0}^{AB}(q+p)G_{\downarrow0}^{(0)B}(p)F_{B\downarrow}L_\downarrow^{AB}(-p)\Big], \tag{11}$$

where

$$L_\sigma^{FF}(p) = (V_\mathbf{p}+W_\mathbf{p})^2 G_{0\sigma,0\sigma}^{\alpha\alpha}(p) + (V_\mathbf{p}-W_\mathbf{p})^2 G_{0\sigma,0\sigma}^{\beta\beta}(p) - \left(V_\mathbf{p}^2 - W_\mathbf{p}^2\right)\left[G_{0\sigma,0\sigma}^{\alpha\beta}(p) + G_{0\sigma,0\sigma}^{\beta\alpha}(p)\right], \tag{12}$$

$$L_\sigma^{GG}(p) = (V_\mathbf{p}+W_\mathbf{p})^2 G_{0\sigma,0\sigma}^{\alpha\alpha}(p) + (V_\mathbf{p}-W_\mathbf{p})^2 G_{0\sigma,0\sigma}^{\beta\beta}(p) + \left(V_\mathbf{p}^2 - W_\mathbf{p}^2\right)\left[G_{0\sigma,0\sigma}^{\alpha\beta}(p) + G_{0\sigma,0\sigma}^{\beta\alpha}(p)\right], \tag{13}$$

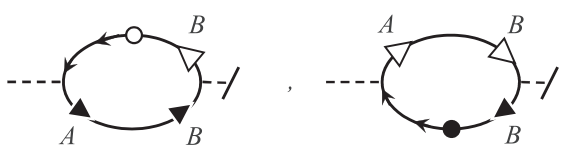

FIG. 3. One-loop diagrams for the AB-components of the force operator of the transverse spin Green's function.

$$L_\sigma^{GF}(p) = (V_{\mathbf{p}} + W_{\mathbf{p}})^2 G^{\alpha\alpha}_{0\sigma,0\sigma}(p) - (V_{\mathbf{p}} - W_{\mathbf{p}})^2 G^{\beta\beta}_{0\sigma,0\sigma}(p) - \left(V_{\mathbf{p}}^2 - W_{\mathbf{p}}^2\right)\left[G^{\alpha\beta}_{0\sigma,0\sigma}(p) - G^{\beta\alpha}_{0\sigma,0\sigma}(p)\right], \quad (14)$$

$$L_\sigma^{FG}(p) = (V_{\mathbf{p}} + W_{\mathbf{p}})^2 G^{\alpha\alpha}_{0\sigma,0\sigma}(p) - (V_{\mathbf{p}} - W_{\mathbf{p}})^2 G^{\beta\beta}_{0\sigma,0\sigma}(p) + \left(V_{\mathbf{p}}^2 - W_{\mathbf{p}}^2\right)\left[G^{\alpha\beta}_{0\sigma,0\sigma}(p) - G^{\beta\alpha}_{0\sigma,0\sigma}(p)\right]. \quad (15)$$

In the above expressions, the summation is carried over the four-momentum $p = (\mathbf{p}, i\omega_n)$, where $i\omega_n$ are the odd Matsubara frequencies. The functions $G^{AB}_{0\sigma,0\sigma}(p)$ and $G^{\nu\mu}_{0\sigma,0\sigma}(p)$ ($A, B = F, G$; $\nu, \mu = \alpha, \beta$) are the propagators for localized and itinerant electrons, respectively. In the Hubbard-I approximation, $G^{(0)A}_{0\sigma}$ are the bare Green's function for the localized electrons of different sublattices. It can be seen that the expressions for the mass and force operators also include the propagators $G^{AB}_{0\sigma,0\sigma}(p)$ and the bare functions $G^{(0)A}_{0\sigma}$, which were defined using the creation operator of localized Hubbard fermions with the spin σ as their generating operator. To calculate this set of propagators, it is convenient to use the relation for the Green's functions

$$D^{AB}_{\sigma 0,\sigma 0}(p) = -D^{BA}_{0\sigma,0\sigma}(-p). \quad (16)$$

Let us introduce the notation

$$d_{AB}(q) = \Sigma^{AB}(q) + J_{\mathbf{q}}\delta P^{A\bar{B}}(q)/2, \quad (17)$$

$$K_{AB}(q) = \delta P^{AB}(q) K_{\mathbf{q}}/2, \quad (18)$$

where $\bar{F} \equiv G$ and $\bar{G} \equiv F$. FF and GG components of the force operator account for the bare end-factors and the corrections due to the hybridization interaction: $P^{FF} = 2R + \delta P^{FF}$, $P^{GG} = -2R + \delta P^{GG}$. Taking into account the mass and force operators we obtain the following expression for the inverse matrix $\hat{G}_\perp^{-1}$ in question:

$$\hat{G}_\perp^{-1} = \begin{bmatrix} i\omega_l - 2\tilde{h} - d_{FF} & -K_{FG} & -J_{\mathbf{q}}R - d_{FG} & -K_{\mathbf{q}}R - K_{FF} \\ -K_{FG} & i\omega_l - 2\tilde{h} - d_{FF} & -K_{\mathbf{q}}R - K_{FF} & -J_{\mathbf{q}}R - d_{FG} \\ J_{\mathbf{q}}R - d_{GF} & K_{\mathbf{q}}R - K_{GG} & i\omega_l + 2\tilde{h} - d_{GG} & -K_{GF} \\ K_{\mathbf{q}}R - K_{GG} & J_{\mathbf{q}}R - d_{GF} & -K_{GF} & i\omega_l + 2\tilde{h} - d_{GG} \end{bmatrix}.$$

Thus, the denominator of the Green's functions can be represented as

$$\Delta(q) = \left[\left(i\omega_l - 2\tilde{h} - d_{FF} - K_{FG}\right)\left(i\omega_l + 2\tilde{h} - d_{GG} - K_{GF}\right) + (J_{\mathbf{q}}R + K_{\mathbf{q}}R + K_{FF} + d_{FG})(J_{\mathbf{q}}R + K_{\mathbf{q}}R - K_{GG} - d_{GF})\right] \times \left[\left(i\omega_l - 2\tilde{h} - d_{FF} + K_{FG}\right)\left(i\omega_l + 2\tilde{h} - d_{GG} + K_{GF}\right) + (K_{\mathbf{q}}R - J_{\mathbf{q}}R + K_{FF} - d_{FG})(K_{\mathbf{q}}R - J_{\mathbf{q}}R - K_{GG} + d_{GF})\right]. \quad (19)$$

4. Spin-charge renormalization of the magnetic excitation spectrum

The spin-wave spectrum is determined by the poles of the Matsubara Green's function (5) after the analytic extension. Therefore, the equation defining the spectrum of the spin-wave excitations in the AFM phase is given by $\Delta(\mathbf{q}, \omega) = 0$. Its important property is associated with the satisfiability of the Goldstone theorem: $\Delta(\mathbf{q} = 0, \omega = 0) = 0$.

Let us demonstrate the existence of the Goldstone boson in the mixed-valence regime under developed spin and charge fluctuations. It is easy to verify the following relations between the components of the mass and force operators: $\Sigma^{AB}(0) = -\Sigma^{AB}(0)$, $\delta P^{AB}(0) = -\delta P^{AB}(0)$. Given this, we obtain

$$\Delta(\mathbf{q} = 0, \omega = 0) = \Sigma^{FF}(0) - \Sigma^{FG}(0) - \left(\frac{J_0 + K_0}{2}\right)\left[\delta P^{FF}(0) - \delta P^{FG}(0)\right] = 0. \quad (20)$$

It is essential that the above equation was obtained without the use of any approximation. In the absence of the exchange interaction ($J = 0$, $K = 0$) the satisfiability of the Goldstone theorem follows from the fact that, as shown by numerical calculations, the equation $\Sigma^{FF}(0) = \Sigma^{FG}(0)$ for the mass operator component holds for all parameters. This corresponds to the case where the AFM ordering mechanism involves only low-energy hybridization processes (see the diagrams in Fig. 2).

If the exchange interaction is non-zero, it renormalizes bare energies of the localized electrons in different sublattices ξ_σ^F, ξ_σ^G and $\Sigma^{FF}(0) \neq \Sigma^{FG}(0)$. Nevertheless, Eq. (20) holds for any parameters since in this case, vanishing of the right-hand side of the equation is achieved due to the finite contributions of the force operator components. This implies the importance of taking into account the force operator, originating from the kinematic interaction of Hubbard fermions. In this case, it is necessary to take into account the graphs of the same order (e.g., only one-loop graphs) both for the mass and force operators in the ensemble of Hubbard fermions as the failure to satisfy this requirement would lead to a breach of the Goldstone theorem.

In what follows, in the calculation of the spectrum of spin-wave excitations, it is sufficient to consider only the hybridization processes between the localized and itinerant electrons in the one-loop approximation. At the same time, in order not to exceed the accuracy of the calculations, in the expressions for the components of the mass and force operators, we use the energy determined without taking into account the hybridization effects as a magnon energy

$$\Sigma^{AB}(q) \to \Sigma^{AB}(\mathbf{q}, \omega_{0i}(\mathbf{q})), \delta P^{AB}(q) \to \delta P^{AB}(\mathbf{q}, \omega_{0i}(\mathbf{q})),$$

where

$$\omega_{01,2}(\mathbf{q}) = R\gamma_{01,2}(\mathbf{q}), \quad \gamma_{01,2}(\mathbf{q}) = \sqrt{(J_0 + K_0)^2 - (J_\mathbf{q} \pm K_\mathbf{q})^2}. \tag{21}$$

The terms of the dispersion equation, containing the product of the components of the mass and force operators are not included. As a result, the spectrum of spin-wave excitations with the spin-charge fluctuations taken into account is determined by the analytical expression

$$\omega_{1,2\mathbf{q}} = \omega_{01,2}(\mathbf{q}) + \delta\omega_{1,2\mathbf{q}}, \tag{22}$$

in which the corrections to the bare spectrum are defined in the form

$$\begin{aligned}\delta\omega_{1,2\mathbf{q}} &= \frac{1}{2}[d_{1,2FF} + d_{1,2GG} \pm (K_{1,2FG} + K_{1,2GF})] - \frac{1}{2\omega_{01,2}(\mathbf{q})} \\ &\times \{(J_0 + K_0)R[d_{1,2GG} - d_{1,2FF} \pm (K_{1,2GF} - K_{1,2FG})] \\ &+ (J_\mathbf{q} \pm K_\mathbf{q})R[d_{1,2FG} - d_{1,2FG} \pm (K_{1,2FF} - K_{1,2GG})]\}.\end{aligned} \tag{23}$$

Here, the following notation was introduced:

$$d_{iAB} = \Sigma^{AB}(\mathbf{q}, \omega_{0i}(\mathbf{q})) + J_\mathbf{q}\delta P^{A\bar{B}}(\mathbf{q}, \omega_{0i}(\mathbf{q}))/2, \tag{24}$$

$$K_{iAB} = K_\mathbf{q}\delta P^{AB}(\mathbf{q}, \omega_{0i}(\mathbf{q}))/2. \tag{25}$$

It turned out that in the case when the localized electron subsystem is close to be completely filled ($n_L \approx 1$), the spectrum of the spin-wave excitations is essentially independent of the hybridization intensity and is determined by the initial expression for the Heisenberg antiferromagnet (21).

The situation is different for the AFM phase if the Fermi level lies in the immediate vicinity of the localized level E_0 and the formation of heavy fermions in the magnetically ordered phase can occur. This state is realized in $CeRhIn_5$ near atmospheric pressure. The spin-wave spectrum for the main direction of the AFM Brillouin zone and the concentration $n_L \approx 0.7$ is shown in Fig. 4. We

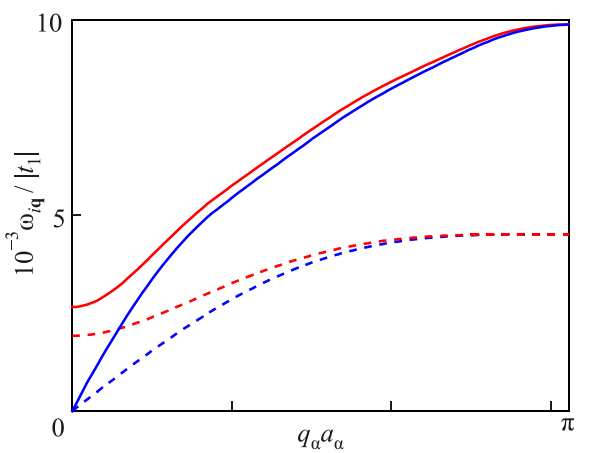

FIG. 4. Spin-wave spectrum of a quasi-two-dimensional structure with the hybridization of localized and itinerant electrons taken into account (solid lines) and the bare spectrum of localized electrons (dashed line) along the direction (111) of the antiferromagnetic Brillouin zone. The concentration of quasi-localized electrons $n_L \approx 0.7$.

introduced the notations: q_α is the component of the wave vector, where $\alpha = x, y, z$; a_α is the corresponding parameter of the unit cell. The dashed lines define the magnon energies $\omega_{0i}(q)$ of the quasi-2D structure without taking into account the processes of hybridization between f- and p-electrons. The solid lines show the ω_{iq} branches of the spin-wave spectrum, taking into account the hybridization interaction with the p-electrons. The interactions parameters were selected as $V = 0.3|t_1|$ (the effective one-site hybridization parameter), $J = 0.004|t_1|$ and $K = J/10$, where t_1 is the hopping parameter between the neighboring sites for the itinerant electrons ($t_1 < 0$). The energy of the f-level $E_0 = 1.5t_1$ and the total concentration of electrons $n_e = 1.2$. From the comparison of the model dispersion relation for itinerant electrons ξ_k and the dispersion relations for In p-electrons in $CeRhIn_5$ obtained from *ab initio* calculations,[34] it follows that $|t_1| \sim 0.1$–0.3 eV. The selected parameters correspond to the spectrum of Fermi excitations shown in Fig. 5. It can be seen that the chemical potential μ (dashed line) crosses the heavy-fermion band with weak dispersion.

These results indicate that in the considered regime, the low-energy hybridization processes lead to a significant increase in the velocity of spin waves κ for the Goldstone mode $\omega_{1q} = \kappa q$ (for small q) and in the magnon energy. In turn, this leads to an increase in the AFM order parameter and the Néel temperature compared to the case of fully localized f-electrons.

The modification of the spin-wave spectrum can be explained by the emergence of additional effective exchange interaction due to low-energy hybridization processes. Indeed, a comparison of Eq. (8), containing the mass operator, and Eq. (9), which takes into account the exchange interaction between the 4f-electrons, shows that the components of the mass operator can be regarded as an effective exchange interaction. Furthermore, the components of the force operator arising due to the hybridization taken into account renormalize the initial value of the AFM order parameter and also affect the magnon energy spectrum.

The parameters of the effective exchange interaction between different lattice sites can be estimated using the equations

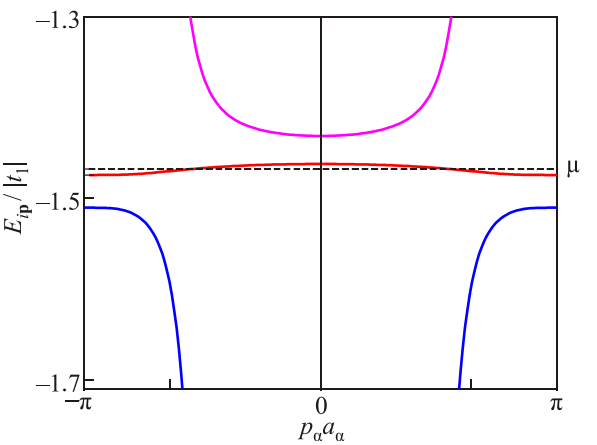

FIG. 5. Spectrum of the Fermi excitations for $n_L \approx 0.7$. The Fermi level is shown with a dashed line.

$$A_{f,g} = \frac{1}{N/2}\sum_{\mathbf{q}} e^{i\mathbf{q}(\mathbf{R}_f - \mathbf{R}_g)}\Sigma^{FG}(\mathbf{q}, \omega_{01}(\mathbf{q})), \tag{26}$$

$$A_{f,f'} = \frac{1}{N/2}\sum_{\mathbf{q}} e^{i\mathbf{q}(\mathbf{R}_f - \mathbf{R}_{f'})}\Sigma^{FF}(\mathbf{q}, \omega_{01}(\mathbf{q})), \tag{27}$$

where the sites denoted with indices f, f' belong to the F-sublattice, and the sites with the indices g belong to the G-sublattice. Note that the effective interaction only occurs between the ions located in the xy-plane since the low-energy hybridization processes are limited to this plane. Thus, the exchange interaction along the z-axis with the parameter K defines the quasi-2D character of the systems studied, while the exchange parameter J in the xy-plane is renormalized by the hybridization interactions. At the same time due to the effective interaction in the xy-plane, the exchange between next-nearest neighbors is also formed.

Qualitatively, the effect of the hybridization of p- and f-electrons on the characteristics of the AFM phase (such as the spin-wave velocity, AFM order parameter and the Néel temperature) is determined by the signs of the parameters $A_{f,g}$ and $A_{ff'}$. If $A_{f,g} > 0$ and $A_{ff'} < 0$, the hybridization processes promote AFM ordering and the spin-wave spectrum takes the form shown in Fig. 5. If the magnon energy decreases when the hybridization is taken into account, the net magnitude of the AFM exchange is reduced due to the frustration when $A_{f,g} < 0$ and $A_{ff'} > 0$. Thus, it is essential that the parameters of the effective interaction depend on the position of the localized level, concentration and temperature.

5. Pressure dependence of the Néel temperature in layered rare-earth intermetallic compounds

The average value of the z-projection of the spin in a sublattice can be calculated using the relations

$$R = n_L/2 - \langle X_{f_1}^{\downarrow\downarrow}\rangle,$$
$$\langle X_{f_1}^{\downarrow\downarrow}\rangle = -\frac{T}{N/2}\sum_{q} e^{-i\omega_n\delta} D_{\perp}^{F_1F_1}(q), \quad \delta \to +0. \tag{28}$$

Substituting the above expression for the transverse spin Green's functions and performing the summation over the Matsubara frequencies, we obtain a self-consistent equation for the order parameter

$$R = \frac{n_L}{2}\left\{\sum_{\mathbf{q}}\left[\frac{2\tilde{h}}{\omega_{1\mathbf{q}}}\frac{2J_{\mathbf{q}}K_{\mathbf{q}}R^2 - A_{1\mathbf{q}}}{\omega_{2\mathbf{q}}^2 - \omega_{1\mathbf{q}}^2}\mathrm{cth}\left(\frac{\omega_{1\mathbf{q}}}{2T}\right) + \frac{2\tilde{h}}{\omega_{2\mathbf{q}}}\frac{2J_{\mathbf{q}}K_{\mathbf{q}}R^2 - A_{2\mathbf{q}}}{\omega_{2\mathbf{q}}^2 - \omega_{1\mathbf{q}}^2}\mathrm{cth}\left(\frac{\omega_{2\mathbf{q}}}{2T}\right) + C_1 + C_2 + \Lambda + \sum_{\mathbf{q}}\frac{2J_{\mathbf{q}}K_{\mathbf{q}}R^2}{\left(\omega_{2\mathbf{q}}^2 - \omega_{1\mathbf{q}}^2\right)}\right.$$
$$\left.\times\left[\frac{1}{\omega_{1\mathbf{q}}}\frac{\Theta_1(\mathbf{q})}{\exp(\beta\omega_{1\mathbf{q}}) - 1} + \frac{1}{\omega_{2\mathbf{q}}}\frac{\Theta_2(\mathbf{q})}{\exp(\beta\omega_{2\mathbf{q}}) - 1}\right]\right\}^{-1}. \tag{29}$$

In writing this equation we used the relations $\Sigma^{AB}(\mathbf{q}, -\omega) = -\Sigma^{AB}(\mathbf{q}, \omega)$ and $\delta P^{AB}(\mathbf{q}, -\omega) = -\delta P^{AB}(\mathbf{q}, \omega)$. For the terms that determine hybridization corrections we introduced the notation

$$A_{i\mathbf{q}} = \omega_{0i}(\mathbf{q})(K_{iFG} + K_{iGF}) + 2\tilde{h}(K_{iFG} - K_{iGF}) - J_{\mathbf{q}}R(K_{iFF} - K_{iGG}) - K_{\mathbf{q}}R(d_{iFG} - d_{iGF}), \quad i = 1, 2, \tag{30}$$

$$C_{1,2} = \sum_{\mathbf{q}}\frac{2J_{\mathbf{q}}K_{\mathbf{q}}R^2}{\omega_{1,2\mathbf{q}}\left(\omega_{2\mathbf{q}}^2 - \omega_{1\mathbf{q}}^2\right)} \times\left[d_{1,2FF} + \frac{1}{2}\left(\gamma_{01,2}(\mathbf{q}) - J_0 - K_0\right)\delta P_{1,2}^{GG} \pm K_{1,2FG} - \frac{1}{2}\left(J_{\mathbf{q}} \pm K_{\mathbf{q}}\right)\delta P_{1,2}^{FG}\right], \tag{31}$$

(here, the "+" and "−"signs correspond to the functions C_1 and C_2, respectively)

$$\Lambda = -\sum_{\mathbf{q}}\frac{1}{\omega_{2\mathbf{q}}^2 - \omega_{1\mathbf{q}}^2}\left[\omega_{01}(\mathbf{q})(d_{1FF} + d_{1GG}) - \omega_{02}(\mathbf{q})(d_{2FF} + d_{2GG}) + 2\tilde{h}(d_{1FF} - d_{1GG}) - 2\tilde{h}(d_{2FF} - d_{2GG}) - J_{\mathbf{q}}R(d_{1FG} - d_{1GF}) + J_{\mathbf{q}}R(d_{2FG} - d_{2GF}) - K_{\mathbf{q}}R(K_{1FF} - K_{1GG}) + K_{\mathbf{q}}R(K_{2FF} - K_{2GG})\right], \tag{32}$$

$$\Theta_{1,2}(\mathbf{q}) = d_{1,2FF} - d_{1,2GG} \pm (K_{1,2FG} - K_{1,2GF}) - \frac{1}{2}\left(J_{\mathbf{q}} \pm K_{\mathbf{q}}\right)\left(\delta P_{1,2}^{FG} - \delta P_{1,2}^{GF}\right) + \frac{1}{2}\left\{\left[\gamma_{01,2}(\mathbf{q}) + J_0 + K_0\right]\delta P_{1,2}^{FF} + \left[\gamma_{01,2}(\mathbf{q}) - J_0 - K_0\right]\delta P_{1,2}^{GG}\right\}. \tag{33}$$

Considering Eq. (29) in the limit $R \to 0$, we obtain the expression for the Néel temperature

$$T_N = \frac{(J_0 + K_0)n_L}{4}\left\{\sum_{\mathbf{q}}\left[\frac{4\tilde{h}^2}{\omega_{1\mathbf{q}}^2}\frac{2J_{\mathbf{q}}K_{\mathbf{q}}R^2 - A_{1\mathbf{q}}}{\omega_{2\mathbf{q}}^2 - \omega_{1\mathbf{q}}^2} + \frac{4\tilde{h}^2}{\omega_{2\mathbf{q}}^2}\frac{2J_{\mathbf{q}}K_{\mathbf{q}}R^2 - A_{2\mathbf{q}}}{\omega_{2\mathbf{q}}^2 - \omega_{1\mathbf{q}}^2} + \sum_{\mathbf{q}}\frac{2\tilde{h}J_{\mathbf{q}}K_{\mathbf{q}}R^2}{(\omega_{2\mathbf{q}}^2 - \omega_{1\mathbf{q}}^2)} \times\left[\frac{\Theta_1(\mathbf{q})}{\omega_{1\mathbf{q}}^2} + \frac{\Theta_2(\mathbf{q})}{\omega_{2\mathbf{q}}^2}\right]\right\}^{-1}_{T\to T_N, R\to 0}. \tag{34}$$

For the study of the dependence of the Néel temperature T_N on the pressure P, we assume that an increase in pressure leads to an increase in energy E_0 of a $4f$-electron on a Ce positive ion due to an increase in the Coulomb interaction with a negatively charged environment. Since the Coulomb interaction (including the interstitial one) is the highest in these systems, the effect of increasing E_0 dominates the increase in the intensity of hybridization and hopping with increasing pressure.

Experimental data for cerium quasi-2D heavy-fermion antiferromagnets, such as $CeRhIn_5$, indicate that in a sufficiently wide range of pressures the Neel temperature decreases linearly with increasing pressure.[3] At the critical pressure, the Neel temperature vanishes and the long-range

AFM order is destroyed. Note that the Neel temperature in these materials does not exceed a few Kelvin.

Figure 6 shows the dependence of the Neel temperature on the bare energy of a 4*f*-electron (pressure) for $V = 0.3|t_1|$, $J = 0.004|t_1|$, $K = J/10$. The dots show the dependence obtained by numerical solution of Eq. (29), taking into account the low-energy hybridization processes of *f*- and *p*-electrons. This curve separates the regions of existence of the AFM and PM phases. The solid line shows the $T_N(P)$ dependence obtained under the assumption of no hybridization interaction in the system. It can be seen that in this case, the Néel temperature decreases linearly with increasing pressure. This behavior is associated with a decrease in the concentration of 4*f*-electrons. The renormalized curve also contains a linear segment at low pressures. At the same time the Néel temperature increases due to the hybridization.

A significant result is that the inclusion of the hybridization interaction between localized and itinerant electrons leads to more rapid destruction of the AFM ordering with increasing pressure. Figure 6 shows that after the range in which there is a slight decrease in the Néel temperature with increasing pressure, the critical region is realized, in which the long-range AFM order is rapidly destroyed. It should be emphasized that without taking into account the spin-charge fluctuations, the $T_N(P)$ dependence would still have a linear character. Therefore, in the developed theory, which takes into account the spin-charge fluctuations, the pressure dependence of the critical AFM temperature is in line with the experimentally observed one. The quantitative agreement with the data on $CeRhIn_5$ is reached for $|t_1| \approx 0.14$ eV. This estimate is reasonable for heavy-fermion systems.

6. Effective exchange interaction with the spin-charge fluctuations taken into account

Figure 7 shows the dependence of the effective exchange integral on the coordination sphere number N_{cs}, calculated according to Eqs. (26) and (27) at a temperature close to zero for two cases: $E_0 = 1.5t_1$ (dots) and $E_0 = 1.21t_1$ (squares). In this case, the coefficient related to the end factor is excluded. Note that upon realization of the long-range

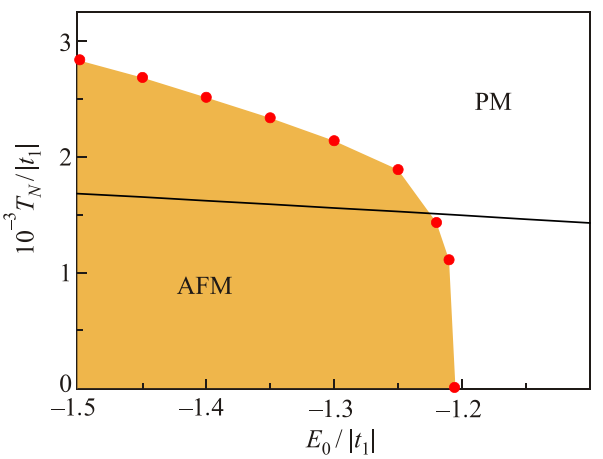

FIG. 6. Dependence of the Néel temperature on the bare energy of localized states (pressure) with (dots) and without (solid line) taking into account the hybridization. Highlighted is the region where the antiferromagnetic (AFM) phase is realized, the rest of the region in the figure corresponds to the paramagnetic (PM) phase.

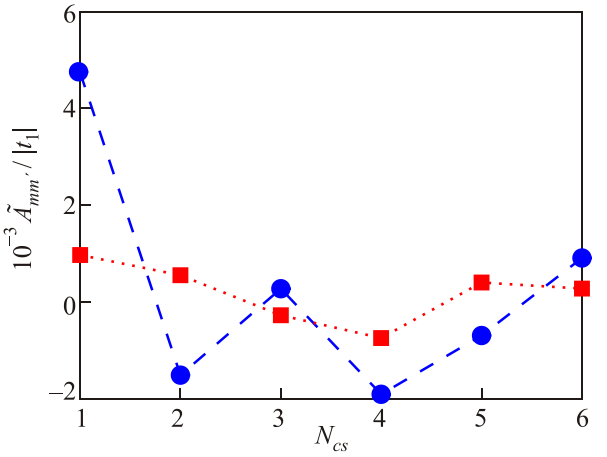

FIG. 7. Dependence of the integral of the effective exchange interaction on the coordination sphere number N_{cs} for two positions of the localized level: $E_0 = 1.5t_1$ (dots) and $E_0 = 1.21t_1$ (squares).

AFM ordering, the exchange interaction in the 1st, 4th and 6th coordination spheres of the square lattice corresponds to the exchange between the AFM sublattices. Accordingly, the interaction in the 2nd, 3rd and 5th coordination spheres characterizes the exchange within the sublattices. Figure 7 shows that for $E_0 = 1.5t_1$, the exchange parameter $\tilde{A}_1$ for the first coordination sphere exceeds by several times the exchange parameters for other neighbors. The total magnitude of the exchange interaction between the nearest ions in the *xy*-plane has the form: $J_{eff} = J + \tilde{A}_1$. Considering the exchange only between the nearest neighbors (with the parameters J_{eff} in the *xy*-plane and *K* along the *z*-axis) in the analytical equation for the Neel temperature of a quasi-2D Heisenberg antiferromagnet with the *f*-level partially filled leads to the estimate $T_N \approx 0.003|t_1|$, which agrees well with the numerical value obtained by solving the self-consistent equations. Thus, the appearance of the effective exchange interaction qualitatively explains the modification of the spin-wave spectrum shown in Fig. 4 and an increase in the Néel temperature. It should be however stressed that the spin-charge fluctuations in the system lead to the frustrated exchange interactions for $N_{cs} = 3$ and 4.

In the critical region with $E_0 = 1.21t_1$, the values $A_{mm'}$ for the nearest and next-nearest neighbors are slightly different from each other and have the same sign. This indicates an increased frustration in the system and the suppression of AFM ordering due to the spin-charge fluctuations in the subsystems of 4*f*- and *p*-electrons. The velocity of spin waves in the critical region is reduced due to these fluctuations. The spin-wave spectrum for $E_0 = 1.21t_1$ takes the form characteristic of the case where the energy of spin-wave excitations falls into the region of the Stoner excitations.

It should be also noted that for both cases the situation is possible when the parameter $A_{mm'}$ increases with the distance $|\mathbf{R}_m - \mathbf{R}_{m'}|$. In this respect, taking into account the effective exchange interaction between distant neighbors can be significant.

It should be emphasized that the above analysis of the effect of spin-charge fluctuations on the effective exchange parameters is qualitative in nature. This is due to the fact that, firstly, the components of the mass operator are temperature dependent. This fact is taken into account in solving

the self-consistent equations, but in the above considerations the exchange parameters at $T = 0$ were used. Secondly, the calculation of the integral $A_{mm'}$ does not explicitly take into account the hybridization corrections in the force operator.

The effects of spin-charge fluctuations in the layered heavy-fermion antiferromagnets, described in this paper, also occur in compounds with the effective interaction of the three-dimensional nature, such as $CeIn_3$. However, in the description of these compounds it is not possible to be restricted to the hybridization and hopping only in the *xy*-plane. In addition, in cerium intermetallic compounds the formation of the phase involving the coexistence of antiferromagnetism and superconductivity near the quantum critical point is of great interest. In the proposed model, the exchange interaction between 4*f*-electrons is capable of inducing the Cooper instability.[35] Then the formation of superconductivity near the quantum critical point is not related to the quantum fluctuations but is due to the suppression of the Cooper pairing by antiferromagnetism. However, these questions are beyond the scope of this paper.

7. Conclusion

Within the framework of the periodic Anderson model, using the diagram technique for Hubbard operators, we developed a theory that allowed us to take into account the spin-charge fluctuations and study the mutual influence of the two microscopic mechanisms of the exchange interaction between the *f*-electrons in quasi-2D cerium heavy-fermion intermetallic compounds.

The first mechanism, which is realized for large values of the intra-atomic Coulomb repulsion, is caused by high-energy hybridization processes between the itinerant *p*-electrons and *f*-electrons of the rare-earth ions. The intensity of the exchange coupling due to this mechanism does not depend on the temperature, concentration of the itinerant carriers and the position of the chemical potential.

For the second mechanism, induced by the low-energy hybridization processes between the above groups of electrons, the situation is qualitatively different. The contribution of these processes to the magnitude of the resulting exchange coupling between Ce ions depends strongly on the position of the Fermi level, energy of the *f*-level and the density of states. This conclusion follows from the analysis of the magnetization behavior of the antiferromagnetic sublattice and the Neel temperature obtained with the contribution of spin-charge fluctuations taken into account. It has been demonstrated that the inclusion of the second mechanism is crucial for the quantitative description of the experimental data, such as the pressure dependence of the Neel temperature obtained for quasi-2D cerium systems (such as $CeRhIn_5$).

This work was supported by RFBR (Grants Nos. 16-02-00073-a and 15-42-04372-r-Siberia-a), the Government of the Krasnoyarsk Region and the Regional Science Foundation (Ext. Agreement No. 07/16), as well as the Integrated program II.2P of SB RAS (Project No. 0358-2015-0002). One of the authors (A.O.Z.) acknowledges the support by the Presidential scholarships for young PhDs (SP-1370.2015.5).

[a]Email: vvv@iph.krasn.ru

[1]Ph. Gegenwart, Q. Si, and F. Steglich, Nat. Phys. **4**, 186 (2008).
[2]N. D. Mathur, F. M. Grosche, S. R. Julian, I. R. Walker, D. M. Freye, R. K. W. Haselwimmer, and G. G. Lonzarich, Nature **394**, 39 (1998).
[3]T. Park and J. D. Thompson, New J. Phys. **11**, 055062 (2009).
[4]E. D. Bauer, H. O. Lee, V. A. Sidorov, N. Kurita, K. Gofryk, J.-X. Zhu, F. Ronning, R. Movshovich, J. D. Thompson, and T. Park, Phys. Rev. B **81**, 180507 (2010).
[5]S. Doniach, Physica B+C **91**, 231 (1977).
[6]P. Coleman, C. Pepin, Q. Si, and R. Ramazashvili, J. Phys.: Condens. Matter **13**, R723 (2001).
[7]Q. Si, S. Rabello, K. Ingersent, and J. L. Smith, Nature **413**, 804 (2001).
[8]H. Shishido, R. Settai, H. Harima, and Y. Ōnuki, J. Phys. Soc. Jpn. **74**, 1103 (2005).
[9]G. Knebel, D. Aoki, J.-P. Brison, and J. Flouquet, J. Phys. Soc. Jpn. **77**, 114704 (2008).
[10]K. Miyake and S. Watanabe, J. Phys. Soc. Jpn. **83**, 061006 (2014).
[11]H. Watanabe and M. Ogata, Phys. Rev. Lett. **99**, 136401 (2007).
[12]S. Watanabe and K. Miyake, J. Phys. Soc. Jpn. **79**, 033707 (2010).
[13]V. V. Val'kov and A. O. Zlotnikov, JETP **116**, 817 (2013) [Zh. Eksp. Teor. Fiz. **143**, 941 (2013) (in Russian)].
[14]E. A. Zhukovskii and V. V. Tugushev, JETP **84**, 330 (1997) [Zh. Eksp. Teor. Fiz. **111**, 600 (1997) (in Russian)].
[15]H. Leder and B. Mühlschlegel, Z. Phys. B **29**, 341 (1978).
[16]B. Möller and P. Wölfle, Phys. Rev. B **48**, 10320 (1993).
[17]R. Doradziński and J. Spałek, Phys. Rev. B **58**, 3293 (1998).
[18]M. E. Foglio, J. Phys. C: Solid State Phys. **11**, 4171 (1978).
[19]P. S. Riseborough and D. L. Mills, Phys. Rev. B **21**, 5338 (1980).
[20]Y. Kuramoto, Z. Phys. B **40**, 293 (1981).
[21]Y. A. Izyumov and B. M. Letfulov, J. Phys.: Condens. Matter **2**, 8905 (1990).
[22]V. V. Val'kov and D. M. Dzebisashvili, Theor. Math. Phys. **164**, 1089 (2010). [Teor. Mat. Fiz. **164**, 309 (2010) (in Russian)].
[23]J. D. Thompson and Z. Fisk, J. Phys. Soc. Jpn. **81**, 011002 (2012).
[24]V. V. Val'kov and A. D. Fedoseev, Theor. Math. Phys. **168**, 1216 (2011). [Teor. Mat. Fiz. **168**, 417 (2011) (in Russian)].
[25]P. Das, S.-Z. Lin, N. J. Ghimire, K. Huang, F. Ronning, E. D. Bauer, J. D. Thompson, C. D. Batista, G. Ehlers, and M. Janoschek, Phys. Rev. Lett. **113**, 246403 (2014).
[26]M. Yashima, H. Mukuda, Y. Kitaoka, H. Shishido, R. Settai, and Y. Ōnuki, Phys. Rev. B **79**, 214528 (2009).
[27]V. V. Val'kov and D. M. Dzebisashvili, Theor. Math. Phys. **157**, 1565 (2008) [Teor. Mat. Fiz. **157**, 235 (2008) (in Russian)].
[28]R. O. Zaitsev, Sov. Phys. - JETP **41**, 100 (1975) [Zh. Eksp. Teor. Fiz. **68**, 207 (1975) (in Russian)].
[29]R. O. Zaitsev, *Diagrammatic Methods in the Theory of Superconductivity and Ferromagnetism* (Editorial URSS, Moscow, 2004) [in Russian].
[30]V. G. Baryakhtar, V. N. Krivoruchko, and D. A. Yablonsky, Sov. Phys. - JETP **58**, 351 (1983) [Zh. Eksp. Teor. Fiz. **85**, 601 (1983) (in Russian)].
[31]V. G. Baryakhtar, V. N. Krivoruchko, and D. A. Yablonsky, *Green's Functions in the Theory of Magnetism* (Naukova Dumka, Kiev, 1984) [in Russian].
[32]R. O. Zaitsev, Sov. Phys. - JETP **43**, 574 (1976) [Zh. Eksp. Teor. Fiz. **70**, 1100 (1976) (in Russian)].
[33]S. G. Ovchinnikov and V. V. Val'kov, *Hubbard Operators in the Theory of Strongly Correlated Electrons* (Imperial College Press, London, 2004).
[34]S. Elgazzar, I. Opahle, R. Hayn, and P. M. Oppeneer, Phys. Rev. B **69**, 214510 (2004).
[35]V. V. Val'kov and A. O. Zlotnikov, JETP Lett. **95**, 350 (2012) [Pis'ma Zh. Eksp. Teor. Fiz. **95**, 390 (2012) (in Russian)].

Translated by L. Gardt.